Phonon studies of Ni^{2+} in GaAs:evidence for an orthorhombic Jahn-Teller system

1989 J. Phys.: Condens. Matter 1 7277

(http://iopscience.iop.org/0953-8984/1/40/003)

J. Phys.: Condens. Matter 1 (1989) 7277–7293. Printed in the UK

Phonon studies of Ni^{2+} in GaAs: evidence for an orthorhombic Jahn–Teller system†

L J Challis‡, B Salce§, N Butler‡, M Sahraoui-Tahar‡ and W Ulrici‖

‡ Department of Physics, University of Nottingham, Nottingham NG7 2RD, UK

§ Centre d'Etudes Nucleaires, Service des Basses Temperatures, 85X, 38041 Grenoble Cedex, France

‖ Akademie der Wissenschaften der DDR, Zentralinstitut fur Electronenphysik, 1086, Berlin, German Democratic Republic

Received 22 February 1989, in final form 23 May 1989

Abstract. Thermal conductivity measurements have been made from 50 mK to 100 K of Ni-doped GaAs samples containing different proportions of Ni^{+}, Ni^{2+} and Ni^{3+}. Resonant phonon scattering at 300 GHz is assigned to Ni^{2+} ($^3T_1$) and this is supported by studies of photoinduced changes in the Ni^{2+} concentration. The scattering is attributed to tunnelling within the ground state of an orthorhombic Jahn–Teller system. Uniaxial stress measurements show that the levels are very sensitive to both E and T_2 strains and provide values of $V_E b$ and $V_T b$. Data for Cr^{3+} ($^4T_1$) in GaAs, GaP and InP are re-examined in the light of these results. It is proposed that the rich spectrum of resonance frequencies is due to multiple-ion effects caused by ion–ion coupling via the strain field.

1. Introduction

Nickel enters readily into substitutional sites in GaAs and has been observed in three valence states, $Ni^{3+}(3d^7)$, $Ni^{2+}(3d^8)$ and $Ni^{+}(3d^9)$. The Ni^{2+}/Ni^{3+} level is believed to be at $E_v + 0.2$ eV and the Ni^{+}/Ni^{2+} level at $E_c - 0.4$ eV (Clerjaud 1985, Ulrici *et al* 1986 and references therein). The occupation of these levels and hence the concentrations of the three ions is determined by the relative concentrations of Ni and other active impurities present, particularly shallow donors and acceptors.

Information on the ground state of the three ions is still relatively sparse (see references above). Ni^{3+} should have a $^4A_2$ ground state and this is confirmed by EPR (de Wit and Estle 1962, Andrianov *et al* 1977, Kaufmann and Schneider 1980) and APR (Rampton and Saker 1986) but the other two ions should have orbitally degenerate ground states ($Ni^{+}: {}^2T_2$, $Ni^{2+}: {}^3T_1$) and so be subject to Jahn–Teller effects. Ni^{2+} is of particular interest since another T_1 ion, $Cr^{3+}(^4T_1)$, is believed to exhibit strong non-linear Jahn–Teller effects in GaAs, GaP and InP and to be very strongly coupled to phonons (e.g. Challis and de Goër 1982, Butler *et al* 1985, 1986). One of the purposes of the present work was to discover whether Ni^{2+} showed similar behaviour. The only other phonon study of Ni^{2+} is by APR (Rampton and Saker 1986). In addition to the

† This paper is dedicated to the memory of Dr Anne-Marie de Goër who died on December 23, 1988. Her warmth, her enthusiasm and the quality of her work on phonons will long be remembered.

0953-8984/89/407277 + 17 $02.50

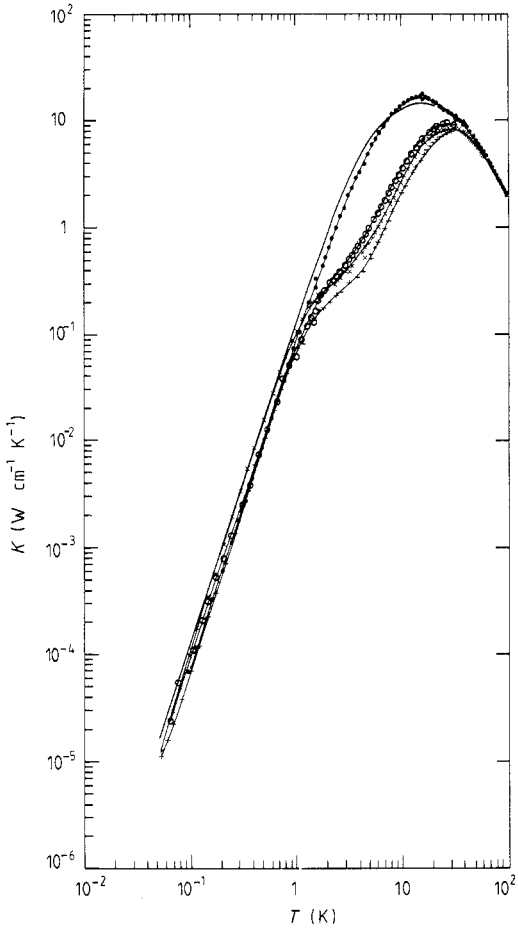

Figure 1. The thermal conductivity of four samples of GaAs: Ni: ●, SN236A1; ○, SN236E1; ×, TN593A; +, TN593E. The curve without data points shows the conductivity of an undoped sample, GA803.

sharp lines due to Ni^{3+} noted above, they observed broad anisotropic resonance absorption which they attributed to Ni^{2+}: the anisotropy suggesting that the ions responsible were distorted or complexed with other centres.

Ni^+, which can be detected by luminescence, is also of interest because of the similarity of its ground state to that of the $^5T_2$ ground state of Cr^{2+} in a T_d site. The tunnelling between the tetragonally placed Jahn–Teller wells of the Cr^{2+} system (Abhvani *et al* 1981, 1982) is believed to be responsible for APR signals in weakly n-type and SI material (e.g. Abhvani *et al* 1983) and for resonant phonon scattering below 5 GHz observed in thermal conductivity (Challis *et al* 1982) and it is of interest to see whether similar effects occur in Ni^+.

We report here thermal conductivity measurements from 50 mK–100 K which provide spectroscopic information in the frequency range 5–1000 GHz. The samples were obtained from LEC grown material and details are given in table 1. The p-type samples TN593A and E were cut from the seed end and tail end respectively of the same boule and the n-type samples. SN236A1 and E1 were cut from a different boule again from the seed and tail ends respectively. The Ni concentrations were obtained by spectrochemical analysis (Ulrici *et al* 1986) and the relative concentrations of Ni^{2+} were determined from the sizes of the optical absorption peaks. Absolute values of $[Ni^{2+}]$ were then obtained

Table 1. Details of the GaAs : Ni samples (A = seed, E = tail end of boule). The samples were grown by the LEC technique. The concentrations of Ni are obtained from spectrochemical analysis whilst Ni^{2+} concentrations are determined from the heights of the optical absorption peaks relative to that for TN593A in which it is assumed [Ni] = [Ni^{2+}]. Concentrations of Mn and Cu are determined by SIMS, which is relatively insensitive to Ni. The values of C, the strength of the resonant phonon scattering at 300 GHz, were obtained from the fits to W/W_0. NA = not available; ND = not detectable.

Sample	Carrier type	Resistivity (Ω mm)	Dimensions (mm^3)	Long axis	[Ni] ($\times 10^{16}\,cm^{-3}$)	[Ni^{2+}] ($\times 10^{16}\,cm^{-3}$)	C ($\times 10^{7}\,s^{-1}$)	[Mn] ($\times 10^{16}\,cm^{-3}$)	[Cr] ($\times 10^{16}\,cm^{-3}$)
SN236A1	n	0.45	18.0 × 2.99 × 3.03	⟨110⟩	0.3	0	0	NA	ND
SN236E1	n	NA	16.1 × 2.59 × 2.98	⟨110⟩	1.2	0.8	0.75	0.65	ND
TN593A	p	1.6×10^5	17.8 × 2.92 × 3.00	⟨100⟩	1.5	1.5	1.2	0.2	0.02
TN593E	p	60	18.2 × 3.00 × 3.00	⟨100⟩	20	2–3	2.2	0.2	0.03

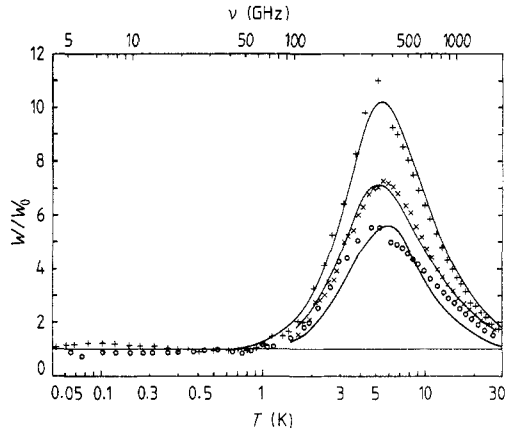

Figure 2. The reduced thermal resistivity W/W_0 of samples: ○, SN236E1; ×, TN593A and +, TN593E. W_0 is the resistivity of SN236A1. The full curves show the ratios of theoretical fits to the data in figure 1.

by assuming that $[Ni^{2+}] = [Ni]$ in TN593A: this is p-type so should contain no Ni^{+} and the Ni^{3+} concentration is evidently small since it gives rise to no detectable EPR signal. Table 1 includes concentrations of Mn and Cr impurities which were obtained by SIMS (Loughborough Consultants).

The measurements of thermal conductivity were made by standard techniques with absolute values accurate to 15% or better; the principal error being in the determination of the separation of the two thermometer contacts (typically 10 ± 1 mm). Measurements of thermal conductivity after optical illumination with sub-bandgap radiation were made using an infrared diode placed 2–3 cm from the sample. The GaAs diode was operated at a current of 15 mA (30 V) and emitted a broad-band spectrum covering the photon energy range 1–2 eV. Illumination was typically for about 10 s. For experiments above 1 K the illumination was performed at 7 K, somewhat above the maximum in the resonant scattering effect seen in the dark (see § 2) and the conductivity was monitored continuously afterwards, for periods up to 3 h. For measurements below 1 K, the illumination was performed at 4 K and the specimen subsequently cooled overnight to mK temperatures. Measurements under compressive uniaxial stress were carried out using the technique used by Ramdane *et al* (1983) and described by Salce (1984). The stress was applied along the long axis of the sample so that measurements for the ⟨100⟩, ⟨111⟩ and ⟨110⟩ directions were made on three different samples cut from neighbouring slices in the boule. The precision of the orientation is believed to be better than 1°. A preliminary report on some of this work has been given by Sahraoui-Tahar *et al* (1989).

2. Orthorhombic Jahn–Teller distortions

The Jahn–Teller behaviour of magnetic ions with a T_1 orbital ground state in a tetrahedral site has been the subject of considerable theoretical attention. If the electron–lattice coupling is weak or modest in strength, the Hamiltonian describing the potential energy of the coupled system is 'linear' to a good approximation. The potential energy surface has minima lying along the ⟨100⟩ and ⟨111⟩ directions and a saddle point along the ⟨110⟩. The Jahn–Teller distortion that occurs is therefore tetragonal or trigonal depending on which minimum lies lowest. However, if the electron–lattice coupling is increased in strength, the Jahn–Teller distortions become larger and the non-linear terms in the Hamiltonian can no longer be neglected. One effect is to lower the energy of the ⟨110⟩

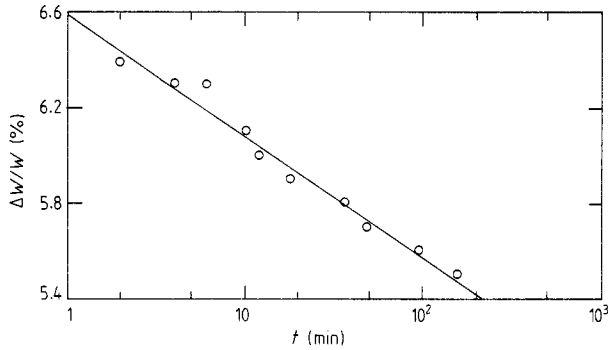

Figure 3. The decay at 7.3 K of the decrease in thermal resistivity ΔW of TN593A produced by illumination. $\Delta W/W$ is the percentage reduction below the value of W before illumination.

saddle-points, until eventually they lie below the lowest minimum (⟨100⟩ or ⟨111⟩) and then turn into energy minima rather than saddle points. When this happens, the Jahn–Teller distortion becomes orthorhombic, although, as in the linear case, the effect of the dynamic terms is to restore the tetrahedral symmetry. The six orbital eigenstates associated with the ⟨110⟩ minima form the representation $T_1 + T_2$ and tunnelling between them splits the two triplets (Muramatsu and Iida 1970, Bersuker and Polinger 1974, Sakamoto 1982, Lister and O'Brien 1984, Bates *et al* 1987). This splitting gives rise to strong resonant scattering at the frequency $4t$ corresponding to the triplet separation.

The Jahn–Teller reduction factors for this system remain large for both E and T_2 symmetry perturbations ($K(E) \sim \frac{1}{4}$, $K(T_2) \sim \frac{1}{2}$ in the strong coupling limit) and only T_1 perturbations, such as spin–orbit interactions, are strongly quenched. This unusual signature, which can be tested by applying ⟨100⟩ (E) and ⟨111⟩ (T_2) uniaxial stress, can also occur when either tetragonal or trigonal wells are lowest, provided the orthorhombic wells are only just above (figure 3 of Lister and O'Brien 1984). However, the strong resonant scattering which should be present in the orthorhombic ground state ($T_1 \rightarrow T_2$) is not present in the tetragonal system which has only one level (figure 2 of Lister and O'Brien) so can be used to distinguish these two cases. The trigonal system with orthorhombic wells just above also has two levels, T_1 and A_2, though these should usually be much further apart than in the orthorhombic case.

3. Experimental results

3.1. Zero stress data

The thermal conductivity (K) of the four Ni-doped samples is shown in figure 1 together with that of an undoped sample GA803 (Challis *et al* 1982). The data for the strongly n-type sample SN236A1 shows no evidence of resonant phonon scattering over the whole temperature range. Below 2 K, its conductivity is proportional to T^3, characteristic of boundary scattering, but is 40 ± 20% lower than that of GA803 which has the same orientation (⟨110⟩) but somewhat larger dimensions, $3.1 \times 3.4 \times 16\ mm^3$, and 10% of the difference is attributable to this.

The data for the three remaining samples are plotted in figure 2 as thermal resistivities, $W = 1/K$, in the reduced form W/W_0 where W_0 is the resistivity of SN236A1.

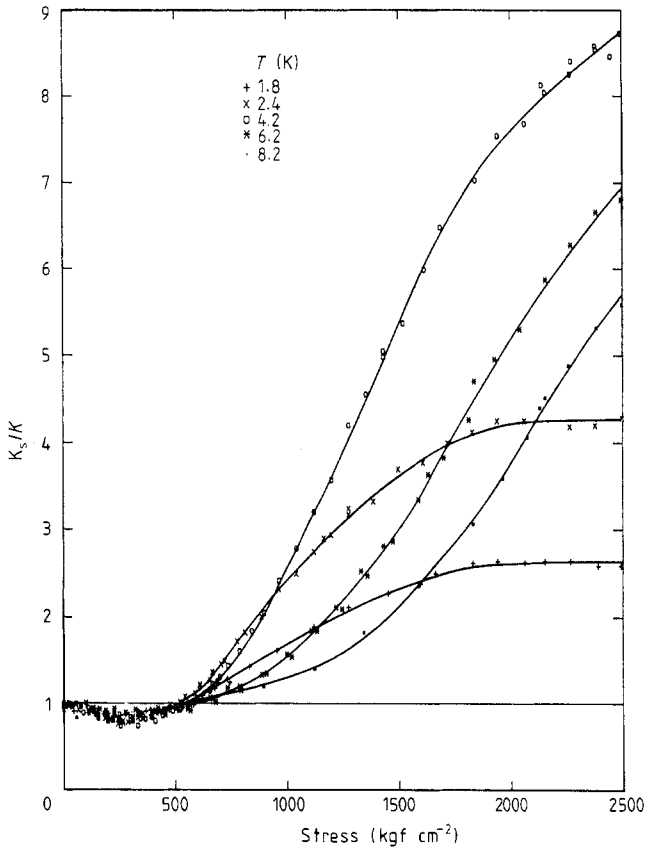

Figure 4. The thermal conductivity of sample TN593E as a function of uniaxial stress along the ⟨100⟩ direction at various temperatures. The data are plotted in the reduced form K_s/K where K is the value in zero stress.

The additional phonon scattering is clearly resonant and attributable to a single centre present in different concentrations in the three samples. Table 1 shows that the weakly n-type sample SN236E1 contains Ni^{+} and Ni^{2+} ([Ni] > [shallow donor] in contrast to SN236A1) and the two p-type samples, TN593A and TN593E, contain Ni^{2+} and a mixture of Ni^{2+} and Ni^{3+} respectively. We assign the resonant scattering to Ni^{2+} since it is the only ion present in all three samples. Figure 2 also shows fits to the data obtained by adding a resonant term $\tau_R^{-1} = C\omega^4/(\omega^2 - \omega_0^2)^2$ to the scattering rate describing the conductivity of SN236A1 ($\tau^{-1} = v/L + A\omega^4 + B_n\omega^2 T^3\ s^{-1}$ with $v/L = 1.5 \times 10^6\ s^{-1}$, $A = 8.6 \times 10^{-45}\ s^3$, $B_n = 1 \times 10^{-22}\ s\ K^{-3}$. The best fits were obtained with $\nu_0 = \omega_0/2\pi =$ 300 ± 30 GHz and the values of C, which should be proportional to the concentrations of the scattering centre, are given in table 1. It is seen that their relative values are consistent with the concentrations of [Ni^{2+}] obtained from the optical absorption peaks adding support to this assignment.

The very weak resonant scattering in TN593E indicated by the small bump in W/W_0 around 100 mK in figure 2 cannot be assigned to Ni^{2+} ions since similar scattering has been seen in three undoped GaAs samples which do not show the Ni^{2+} scattering at 300 GHz (Salce 1989). We note too that there is no evidence of resonant scattering even

at low temperatures in the strongly n-type sample SN236A1 which is only believed to contain Ni^+ ($^2T_2$). This can be compared with the behaviour of Cr^{2+} ($^5T_2$) in GaAs. In this case, no scattering was observed above 100 mK approximately but resonant scattering was apparent below, with its peak at $T < 50$ mK indicating a resonant frequency $\nu_0 \leqslant 5$ GHz attributed to tunnelling between the Jahn–Teller wells. The absence of scattering from Ni^+ above 70 mK very probably suggests that if there is a low-frequency resonance, it must lie well below 5 GHz. However, since random strains are likely to quench the phonon scattering from the majority of ions (Challis *et al* 1982), we cannot totally rule out the possibility that it occurs at higher frequencies but is too weak to see.

3.2. *Effects of optical illumination*

The effect of shining light ($h\nu > 0.5$ eV) onto samples STN593 at low temperatures is known from optical and EPR studies to reduce the Ni^{2+} concentration through the photoinduced recharging process $2Ni^{2+} \rightarrow Ni^{3+} + Ni^+$ (Ulrici *et al* 1986). The effect of this on the phonon scattering was examined by illuminating sample TN593A while at 7.3 K with light at 1.3 eV. The thermal resistivity fell by 30% at saturation (illumination for 2 min) providing further evidence that the phonon scattering is indeed due to Ni^{2+}. At 7.3 K and in the dark, the percentage fall in thermal resistivity $\Delta W/W$ produced by a 10 s light pulse decayed logarithmically with time as shown in figure 3. The form of this decay suggests that recombination occurs by tunnelling (Queisser and Theodorou 1986) and is consistent with that observed by optical absorption (Ulrici and Kreissl 1988).

Measurements below 1 K were made on the n-type sample SN236E1 after illumination but no significant change in conductivity was observed.

3.3. *Effects of uniaxial stress*

Figures 4–6 show the effect on the conductivity of TN593E at various temperatures of uniaxial compressive stress applied along the ⟨100⟩, ⟨111⟩ and ⟨110⟩ directions. The anisotropy of the stress effects at 1.8 K is seen clearly in figure 7. Further data on TN593E and data for TN593A, which are in general very similar to those for TN593E, are given by Sahraoui-Tahar (1988). The rapid changes with stress produced by both ⟨100⟩ and ⟨111⟩ stress indicate that Ni^{2+} is strongly coupled to both E and T_2 strains and from this and the strong resonant scattering at 300 GHz, we conclude that orthorhombic Jahn–Teller effects are present as in Cr^{3+}. At the lowest temperatures, the increase produced by ⟨100⟩ and ⟨111⟩ stress eventually saturates though the saturation value, K_s is 4.5 times larger for ⟨100⟩ than for ⟨111⟩ stress. For ⟨100⟩ stress at 1.8 and 2.4 K, W/W_s ($=K_s/K$) has values of 2.6 and 4.3 respectively which are close to those of $W/W_0 = 3.0 \pm 0.6$ and 5 ± 1 (figure 2) so that $W_s \simeq W_0$, the value for pure GaAs. We conclude that the effect of ⟨100⟩ stress at low temperatures is either to increase the resonant scattering frequency ν_0 to beyond the phonon spectrum ($h\nu_0 \gg kT$), or to quench the scattering or to depopulate the scattering levels. Saturation was not reached at the higher temperatures for the stress range used, although the effects at large stresses still seem consistent with the model: at 4.2 K, W/W_s seems likely to be 9.5–10 and $W/W_0 = 10 \pm 2$. The other feature of the ⟨100⟩ data is a shallow minimum whose position is temperature independent and this will be discussed later. The conductivity is less sensitive to ⟨111⟩ stress and even less to ⟨110⟩ stress except at the lowest temperature where the ⟨110⟩ effects are greater than those for ⟨111⟩. There are no significant minima at low stresses for either of

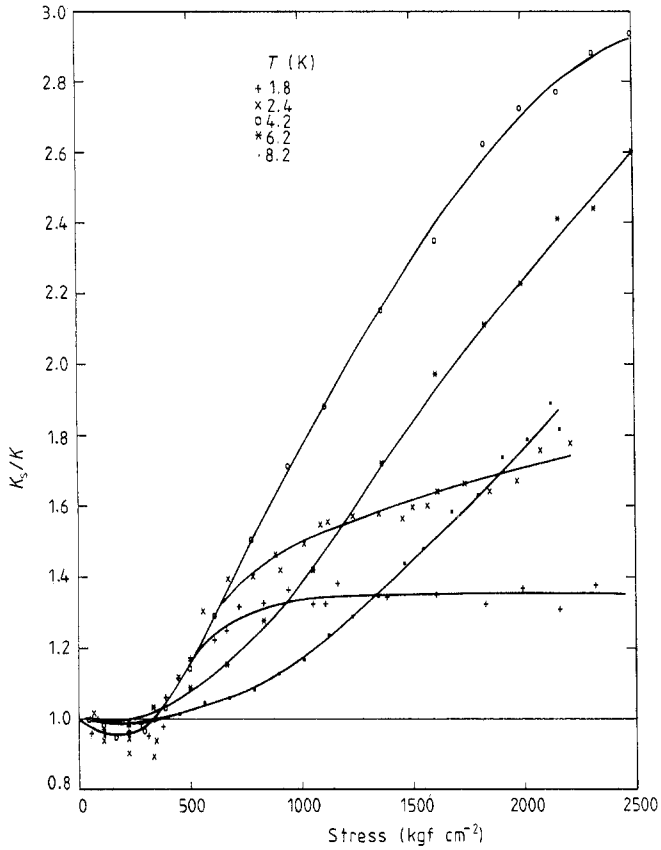

Figure 5. The reduced value of the thermal conductivity K_s/K of sample TN593E as a function of uniaxial stress along the ⟨111⟩ direction at various temperatures.

these two directions. The ⟨110⟩ effects are substantially bigger than those observed for Cr^{3+} in GaAs (Ramdane *et al* 1981, 1983).

4. Discussion

The existence of strong, resonant scattering attributable to Ni^{2+} and the sensitivity of the levels to both E and T_2 strain suggests that this ion is undergoing an orthorhombic Jahn–Teller effect as discussed in § 2. The triplet separation, $4t$, is evidently 300 GHz and figure 8 shows the effect of uniaxial stress calculated from the expressions given by Stauss and Krebs (1980) for $V_E b = 40\,000\ \text{cm}^{-1}$ and $V_T b = \pm 25\,000\ \text{cm}^{-1}$. (Alternative though essentially equivalent expressions in which t is related to the coupling constants have been given recently by Dunn and Bates (1988).) ⟨100⟩ stress leaves a doublet of orthogonal states lowest ($V_E > 0$) while ⟨111⟩ stress, which would not split the $^3T_1$ in the absence of tunnelling, reduces the splitting from $4t$ to $3t$ for both $V_T > 0$ and $V_T < 0$. So large ⟨100⟩ stress takes ν_0 outside the phonon spectrum and depopulates any other scattering levels. This causes the conductivity to rise and saturate at the value for pure GaAs. ⟨111⟩ stress increases the conductivity to a new value consistent with a reduced

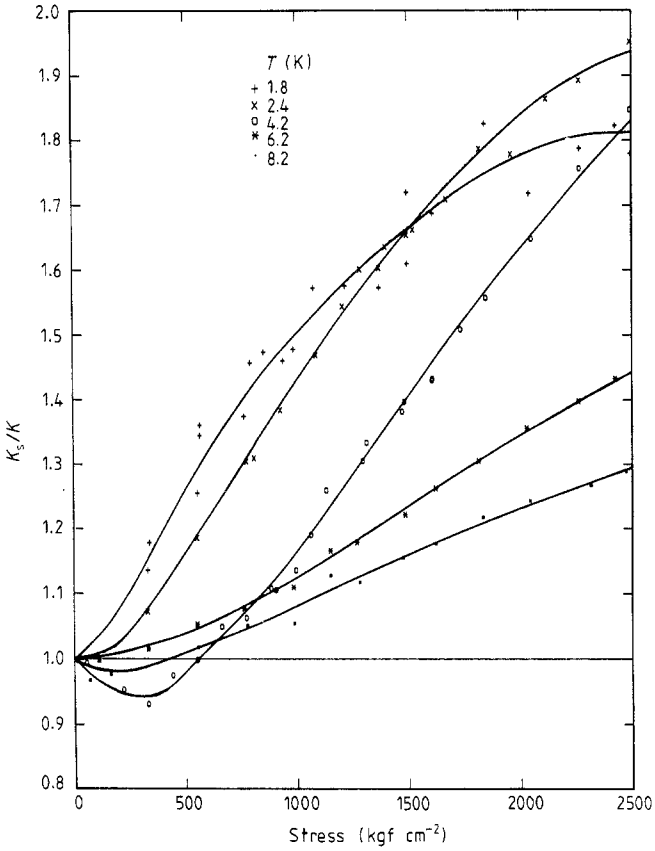

Figure 6. The reduced value of the thermal conductivity K_s/K of sample TN593E as a function of uniaxial stress along the ⟨110⟩ direction at various temperatures.

number of transitions and a change in resonant frequency ($4t \rightarrow 3t$). (The number of transitions, $i \rightarrow j \rightarrow k$ for ⟨100⟩ stress is 27 and for ⟨111⟩ stress is two for $V_T < 0$ and four for $V_T > 0$.) ⟨110⟩ stress leaves four closely spaced levels lowest ($V_E > 0$) and two singlets, and one of the two singlets can lie below, within or above the four closely spaced levels depending on the ratio $|V_T|/V_E$. (The levels are independent of the sign of V_T.) The last two cases would result in rather small changes in conductivity, but when the singlet lies below the other four levels, there is a gradual depopulation of the scattering levels with stress so that the conductivity should rise slowly towards the pure value. This requires $|V_T|/V_E > \frac{1}{4}(s_{11} - s_{12})/s_{44}$ or $> \frac{1}{4}$ when $s_{11} - s_{12} \sim s_{44}$ as it does in GaAs though numerical analysis suggests that $|V_T|/V_E$ will need to be greater than $\frac{1}{3}$ to produce significant changes for the conditions used in the present experiments.

This model appears qualitatively consistent with the experimental observations. The conductivity at 1.8 K saturates at high stress with values equal to K_0 and below K_0 for ⟨100⟩ and ⟨111⟩ stresses respectively as predicted. The data suggest that saturation at K_0 might also result from large ⟨110⟩ stress although at values three times those needed for ⟨100⟩ stress, which is also consistent with the model provided that $|V_T|/V_E > \frac{1}{4}$ so that a singlet falls below the other four levels as the stress is increased.

The shallow minimum produced by ⟨100⟩ stress is of note as it differs from minima seen in Cr^{3+} in GaAs, GaP and InP whose positions increase linearly with temperature

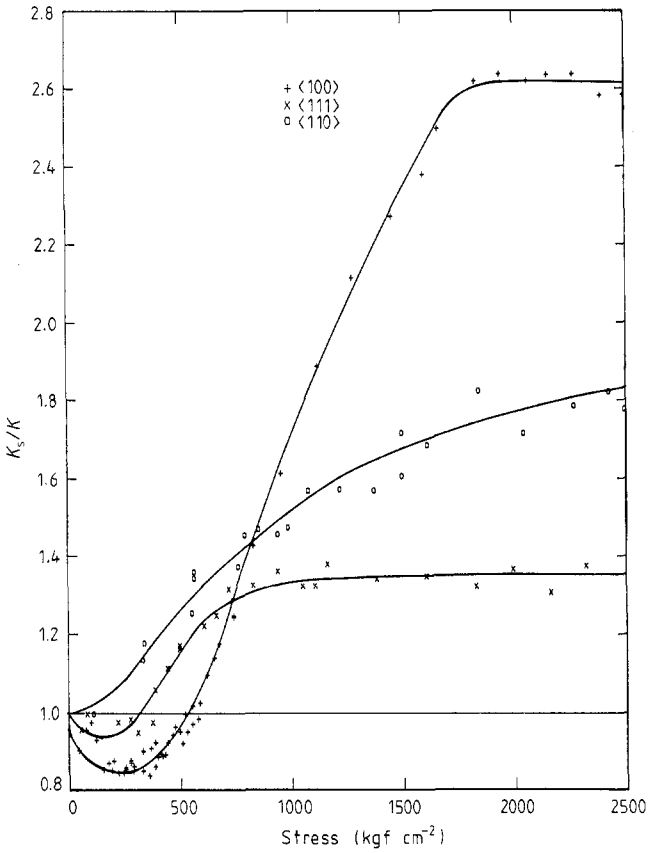

Figure 7. The reduced value of the thermal conductivity K_s/K of sample TN593E as a function of uniaxial stress along the ⟨100⟩, ⟨111⟩ and ⟨110⟩ directions at 1.8 K.

up to 4 K. These minima were attributed to the additional A → E scattering caused by the splitting of the T_1 level. The minimum was thought to occur when the splitting frequency passed through the peak of the phonon spectrum which varies linearly with temperature. The temperature-independent minimum seen in the present data seems attributable to a frequency crossing effect at zero stress (e.g. Berman *et al* 1963). The effect of the $T_1 \rightarrow T_2$ scattering is least when resonant frequencies of the various transitions coincide at zero stress. It increases as the resonant 'holes' from each transition are separated by stress so covering a larger area of the phonon spectrum. The effect should only depend on the stress required to achieve this and so should be independent of temperature. Less pronounced minima are seen for ⟨111⟩ stress and even smaller for ⟨110⟩ stress at the higher temperatures only.

We conclude that the orthorhombic model provides a good qualitative description of the data and, in the next section, we use it to determine the lattice coupling constants.

5. Determination of the lattice coupling constants $V_E b$ and $V_T b$

Figures 9(*a*) and (*b*) show W/W_0 for sample TN593E plotted against temperature for different ⟨100⟩ and ⟨111⟩ stresses respectively (full curves). The plots were obtained

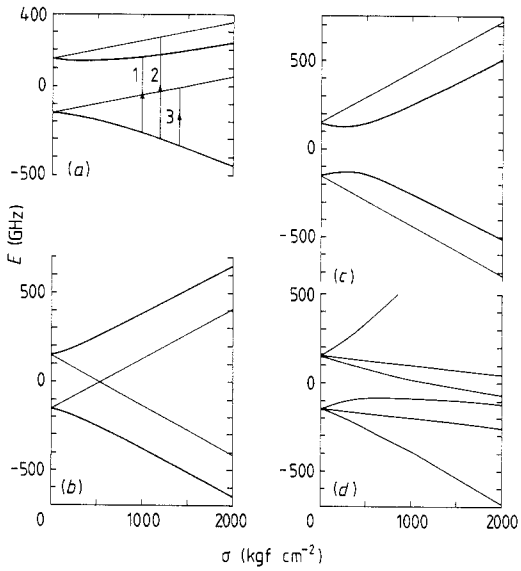

Figure 8. The energy levels calculated for an orthorhombic Jahn–Teller system as a function of uniaxial stress along the three principal directions for $4t = 300$ GHz, $V_E b = 40\,000$ cm^{-1} and $V_T b = \pm 25\,000$ cm^{-1}. The thick lines are doublets. (*a*) ⟨100⟩; (*b*) ⟨111⟩ $V_T > 0$; (*c*) ⟨111⟩, $V_T < 0$; (*d*) ⟨110⟩; levels independent of sign V_T.

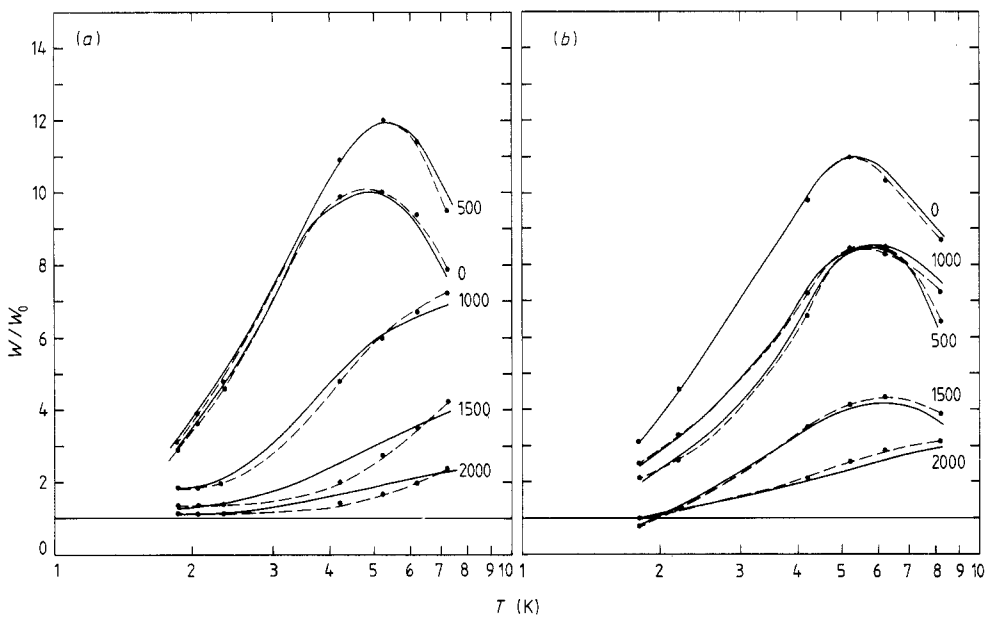

Figure 9. The reduced thermal resistivity W/W_0 of sample TN593E as a function of temperature for different values of stress in kgf cm^{-2}. W_0 is the thermal resistivity of SN236Al. The points and broken curves drawn through them show the experimental data and the full curves show calculated values. (*a*) ⟨100⟩, (*b*) ⟨111⟩.

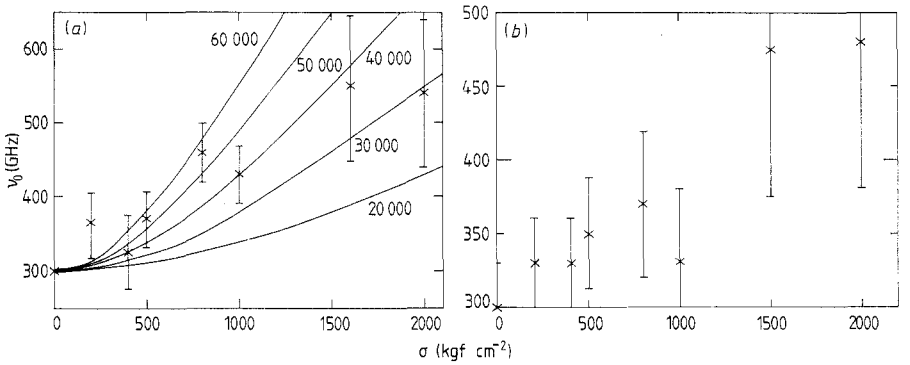

Figure 10. The resonant scattering frequencies obtained from the fits to the data in figure 9 plotted as a function of stress. The full curves are calculated for $4t$ = 300 GHz and different values of $V_E b$ or $V_T b$ in cm^{-1}. (*a*) ⟨100⟩, (*b*) ⟨111⟩.

from the data in figures 4–6, interpolating where necessary. The full curves in the plots show fits to the data made on the assumption that the additional scattering to that in SN236A1 can still be represented by a resonant scattering term of the form used in zero stress but with different values of ω_0 and C. The resonant frequencies ω_0 obtained from these fits are shown in figure 10.

We first consider the data for ⟨100⟩ stress shown in figure 10(*a*) and compare this with the transition frequencies between the energy levels of figure 8. The population of the upper triplet will be negligible at these temperatures and we make the simplifying assumption that the predominant scattering has a resonant frequency close to the separation of the two doublets. There is of course also scattering at a somewhat higher frequency (transition 2) as well as at a lower frequency (transition 3) but it seems reasonable to suppose that transition 1 between the two doublets will dominate. The lines in figure 10(*a*) show the stress dependence of this frequency for a range of values of $V_E b$ and comparison with the experimental data suggests that $V_E b = 40\,000 \pm 15\,000$ cm^{-1}. The energy levels were calculated from the expressions given by Stauss and Krebs (1980) assuming $s_{11} - s_{12} = 1.51 \times 10^{-11}$ m^2 N^{-1} and that the Jahn–Teller reduction factor $K(\mathrm{E})$ had its limiting value of $\frac{1}{4}$. We conclude that $V_E b > 0$ since the conductivity would not saturate at high stress at the value for pure GaAs if the order of the levels were reversed.

We next consider the data for ⟨111⟩ stress shown in figure 10(*b*) and compare it with the transition frequencies between the energy levels of figure 8 which are given for positive and negative values of V_T. In both cases, the resonant frequency falls from $4t$ to $3t$ at high stress where we have again neglected the population of the upper levels. This seems broadly consistent with the data points in figure 10(*b*) which suggest a rather weak dependence of ω_0 on stress at least up to 1000 kgf cm^{-2} and to obtain a value of $V_T b$ we return to figure 5 which shows that at 1.8 K saturation is reached at 1000 kgf cm^{-2}. We first consider $V_T < 0$ and in calculating the energy levels we assume $K(\mathrm{T}_2)$ has its limiting value of $\frac{1}{2}$ and take $s_{44} = 1.66 \times 10^{-11}$ m^2 N^{-1} (these values of the elastic constants are from Cottam and Saunders (1973)). The data suggest that $|V_T b| > 20\,000$ cm^{-1} since for this value the separation of the lower two levels at 1000 kgf cm^{-2} is only 79% of $3t$ so that saturation is still incomplete. The stress dependence above 1000 kgf cm^{-2} at 2.4 K suggests that scattering to the upper levels cannot be totally negligible, indicating that

at 1000 kgf cm^{-2}, the nearest level must be less than 15 kT or 720 GHz above the ground state and this requires $|V_T b| \leqslant 30\,000$ cm^{-1}. So together these results suggest that $|V_T b| \sim 25\,000$ cm^{-1}, the value used in figure 8. A similar analysis for $V_T > 0$ leads to approximately the same value and the temperature dependence of the data above 1000 kgf cm^{-2} appears to be in somewhat better agreement with this case for which the upper levels are closer to the ground state. The values of V_E and V_T are consistent with the requirement that $|V_T|/V_E > \frac{1}{4}$ as required by the ⟨110⟩ stress data and a closer check can be made by noting that, at 1.8 K, the conductivities under ⟨110⟩ and ⟨111⟩ stress are not very different at 1000 kgf cm^{-2} (figure 7). Now since the numbers of transitions involved in the resonant scattering are also similar (two or four for ⟨111⟩ and one for ⟨110⟩ plus three more of increasing frequency and so decreasing effect on the conductivity) the excitation energy of the first excited state in the ⟨110⟩ case must also be close to $3t = 225$ GHz as in the ⟨111⟩ case and for the values of coupling constants given above we obtain 190 GHz. We conclude that $V_E b = 40\,000 \pm 15\,000$ cm^{-1} and $V_T b = 25\,000 \pm 10\,000$ cm^{-1} provide a reasonable account of the stress data for all three directions and note that there is some evidence that $V_T b$ may be positive.

Further information on the strength of the coupling can be obtained from the average value of the phonon matrix element M between the $^3T_1$ and $^3T_2$ levels. The expression $\tau_R^{-1} = C\omega^4/(\omega^2 - \omega_0^2)^2$ found to give a good description of the scattering in zero stress characteristic of the second-order (elastic) process for which $C = C'N\omega_0^2\bar{M}^4/\pi\hbar^2\rho^2 v^7$ approximately (e.g. Challis and de Goër 1984; C' depends on the details of the coupling but seems to lie between 1 and 10). We take $C' = 3$, $v = 3.3 \times 10^3$ m s^{-1} and for sample TN593A, for which the concentration N is known best, we obtain $\bar{M} = 7000$ cm^{-1} which is similar in magnitude to the values of $K(E)V_E b$ and $K(T_2)V_T b$ as expected.

6. A Ni^{2+} complex?

The absence of phonon scattering below 1 K associated with Ni^{2+} is in marked contrast with V^{2+} in GaAs (Butler *et al* 1989a) and Ni^{2+} and V^{2+} in GaP (Butler *et al* 1989b). In these three systems, there is a peak in W/W_0 at around 0.1–0.2 K indicating resonant scattering at ~10–20 GHz which we attribute to the T_1 system in complex with a defect. It would seem therefore either that the Ni^{2+} complex, if it exists in GaAs, differs markedly from these other systems or that it does not exist in the particular samples that we have examined. This could be the case if the Ni^+ complex/Ni^{2+} complex level were below that of Ni^+/Ni^{2+} as is the case for the Ni donor complexes (Ennen *et al* 1981) so that all the complex was in the Ni^{2+} state in the two n-type samples and, if the Ni^{2+} complex/Ni^{3+} complex level were above that of Ni^{2+}/Ni^{3+} so that all the complex was in the Ni^{3+} state in the p-type samples. If this were the case, one might expect to see photoproduction of the Ni^{2+} complex but, as reported in § 3.2, no effects were seen in the conductivity of the n-type sample SN236E1 below 1 K following low temperature illumination. We recall, however, that in the technique used in this range the measurements were made 15–20 h after illumination so would only be sensitive to persistent centres.

7. Conclusion

Thermal conductivity measurements show strong resonant scattering at 300 GHz due to Ni^{2+} ions. The conductivity is sensitive to both E and T_2 strains and the results

are consistent with an orthorhombic Jahn–Teller model with tunnelling frequency $4t = 300$ GHz. The stress dependence leads to values of the coupling constants of $V_E b = +40\,000 \pm 15\,000\ \text{cm}^{-1}$ and $V_T b = 25\,000 \pm 10\,000\ \text{cm}^{-1}$. There is some evidence that $V_T > 0$.

The absence of resonant phonon scattering from $Ni^+(^2T_2)$ above 5 GHz suggests that the Jahn–Teller tunnelling frequency is less than this and so less than that for $Cr^{2+}(^5T_2)$ though we cannot totally rule out the possibility that it is too weak to be seen because of quenching by random strains.

Acknowledgments

We are very grateful to Mr D Arnaud, Mr J-A Favre and Mr J-M Martinod for making many of the measurements, to Mr W B Roys for preparing many of the samples and to Professor C A Bates and Dr J L Dunn, Dr A M de Goër and Dr M C M O'Brien for very helpful discussions. We are also grateful to the Science and Engineering Research Council and the Royal Society for support, to SERC for the award of a research fellowship (NB), and to the Algerian Ministry of Higher Education and Scientific Research and the British Council for a research studentship (MST).

Appendix. Re-examination of data for Cr^{3+} in GaAs, GaP and InP

The observation that the phonon scattering by Ni^{2+} in GaAs occurs at a single frequency is in agreement with the orthorhombic model as we have seen, but is in marked contrast with observations on the T_1 systems, Cr^{3+} in GaAs, GaP and InP which show a complex spectrum of frequencies (Challis *et al* 1982, Ramdane *et al* 1981, 1983, Butler *et al* 1985, 1986). The suggestion by Challis *et al* that this spectrum might be the result of spin–orbit splitting would now seem to be ruled out by the results for GaAs:Ni^{2+}. The spin–orbit coupling constant is smaller in Cr^{3+} than in Ni^{2+} while the quenching of the first-order splitting should be greater in view of the even stronger lattice coupling. We conclude that any splitting should be even smaller for Cr^{3+} than for Ni^{2+} where it appears to be too small for us to detect.

It has been suggested that the lower frequency lines in the spectrum might be due to a complex, Cr^{2+}–X (Austen *et al* 1984) which is believed to be responsible for an optical transition at 0.839 eV (e.g. Barrau *et al* (1983) the defect is attributed to a vacancy; Skolnick *et al* (1982), Fujiwara *et al* (1982)). Austen *et al* showed that the frequencies and intensities seen in phonon scattering are in good agreement with those calculated from their analysis of the Cr^{2+}–X optical data. However, these levels are very sensitive to the parameters of the model and a serious difficulty with this assignment of the phonon scattering to Cr^{2+}–X is to reconcile the very strong scattering with the small concentration of the complex. The arguments for and against this assignment are discussed further by Challis and de Goër (1984).

We propose here an alternative explanation that the complex spectrum is a consequence of the very strong lattice coupling of Cr^{3+} combined with an inhomogeneous distribution of ions within the sample indicated by recent optical data (Ulrici and Kreissl 1988) and that it arises through multiple-ion effects caused by ion–ion coupling via the strain field. This coupling, also described as virtual phonon exchange (VPE), is believed to be the dominant interaction between ions that are strongly coupled to the lattice

(Baker 1971, Gehring and Gehring 1975) and is thought to be responsible for multiple-ion effects seen in the phonon scattering by Cr^{2+} and Mn^{3+} ions in Al_2O_3 which are strongly coupled to the lattice (Hasan *et al* 1979, Zoller *et al* 1980). Thus, in Al_2O_3 samples containing a few PPM of Cr (probably less than 1 PPM of Cr^{2+}), scattering attributable to Cr^{2+} was observed at 200 GHz. But when the Cr concentration was increased to 55 PPM (perhaps less than 10 PPM of Cr^{2+}) strong scattering was also seen at 400 GHz and weak scattering at 600 GHz. This is consistent with the existence of weakly coupled pairs and triads of Cr^{2+} ions.

The effects in GaAs:Cr^{3+} are evidently much more complicatd than those for Cr^{2+} and Mn^{3+} in Al_2O_3 presumably because the strain field from a Cr^{3+} ion produces significant changes in the transition frequencies of its neighbours. Within the orthorhombic model, E strains above some quite modest value, either quench the resonant scattering at $4t$ or add an additional process at $2t$ while T_2 strains reduce the frequency to $3t$. So it seems likely that a cluster of Cr^{3+} ions would scatter phonons at $2t$, $3t$ and $4t$, together with the combination frequencies t, $5t$ etc. This argument considers ions to be subject predominantly to either E or T_2 strains and other transition frequencies may arise when the two types of strain are comparable. The existence of an inhomogeneous distribution of ions would seem to be a necessary feature of this explanation since more than one scattering frequency is present even at quite low Cr^{3+} concentrations (e.g. sample TI4 of Challis *et al* with less than 0.05 PPM Cr^{3+}).

For quantitative comparison, we use the results of tunnel junction phonon spectroscopy on Cr^{3+} in GaAs (Hamdache *et al* 1982), since they are of somewhat higher resolution than those of W/W_0, with which they broadly agree. We add, however, the resonance at 21 GHz seen in W/W_0 which was outside the range of the junctions. This gives a spectrum with resonant frequencies at $\nu_0 = 21, 81, 125, 150, 170, 320, 585(?)$ and 720 GHz. The fine structure around 150 GHz could be due to coupling with the 21 GHz resonance and, if so, the main frequencies would be $\nu_0 = 21$, 81, 150, 320, 585(?) and 720 GHz. The resonances at 80, 150, 320 and 720 GHz could be assigned to an approximate series t, $2t$, $4t$ and $8t$ based on $t \sim 80$ GHz or, if $t \sim 160$ GHz, to a series t, $2t$ and $4t$ with now both the 21 and 80 GHz ascribed to smaller splittings. (The 21 GHz resonance is similar in frequency to that attributed to complexes associated with V^{2+} in GaAs (Butler *et al* 1989a) and Ni^{2+} and V^{2+} in GaP (Butler *et al* 1989), though the strength here seems remarkably strong if this is due to a Cr^{3+} complex.) The relative stability to ⟨100⟩ stress of a transition around 690 GHz (10 K) seen in figure 3 of Ramdane *et al* (1983) might identify this as the tunnelling frequency, $4t$, of the single ion, at a site where the ⟨100⟩ strain is already very large, so favouring the second assignment more. It could evidently be of considerable interest to have a detailed calculation of the spectrum arising from a randomly distributed cluster of interacting ions satisfying the orthorhombic model.

The stress data of Butler *et al* (1985, 1986) and Ramdane *et al* (1983) can be used to re-estimate the values of the lattice coupling constants for Cr^{3+} ions in GaAs, GaP and InP. Because of the more complicated scattering spectra of these systems, it is not possible to use the method used here for Ni^{2+} but it would seem reasonable to obtain values for $V_E b$ and $V_T b$ for Cr^{3+} by comparing the curves for K_s/K for Ni^{2+} in GaAs with those for Cr^{3+}, in particular the values of stress at 50% of saturation. This approach suggests that $V_E b$ is larger for Cr^{3+} than for GaAs:Ni^{2+} by factors of about 2.5 (GaAs), <2 (GaP) and 2.5 (InP); and $V_T b$ by 1.5 (GaAs), 1.0 (GaP), and <1 (InP), so leading to the values for $V_E b$ and $V_T b$ shown in table 2. These values are appreciably smaller than those obtained previously for Cr^{3+} (e.g. GaAs: $V_E b \sim 600\,000$ and $V_T b \sim 150\,000$ cm^{-1})

Table 2. The ion–lattice coupling constants of Cr^{3+}, V_Eb and V_Tb in cm^{-1} calculated from the data of Ramdane *et al* (1983) and Butler *et al* (1985) using the procedure described in the Appendix. The corrected values were obtained by adjusting the values to be consistent with the ratios of $|V_T|/V_E$ indicated by the ⟨110⟩ data.

	GaAs	GaP	InP
Uncorrected			
V_Eb	100 000 ± 40 000	<80 000 ± 30 000	100 000 ± 40 000
V_Tb	40 000 ± 15 000	25 000 ± 10 000	<25 000 ± 10 000
Corrected			
V_Eb	110 000 ± 40 000	80 000 ± 30 000	80 000 ± 40 000
V_Tb	35 000 ± 15 000	25 000 ± 10 000	30 000 ± 10 000

from the positions of the minima at low stresses (Ramdane *et al* 1983, Butler *et al* 1985). We believe the present values to be more soundly based and for Cr^{3+} in GaAs they are in very good agreement with those obtained by EPR: $V_Eb \sim 100\,000$, $V_Tb \sim 35{,}000\ cm^{-1}$ (Stauss and Krebs 1980). (V_Tb for Cr^{3+} GaP is, however, somewhat smaller than that obtained from optical data: $K(T_2)V_Tb = -29\,000\ cm^{-1}$ (Dunn and Bates 1988, from the data of Thomas *et al* 1987) though this analysis assumes a tetragonal Jahn–Teller model.) The values in table 2 need some adjustment within the errors to satisfy the requirements of the ⟨110⟩ data. Thus the absence of ⟨110⟩ stress dependence for Cr^{3+} in GaAs and GaP and the stress dependence for Cr^{3+} in InP suggests adjustment to the corrected values shown.

References

Abhvani A S, Austen S P, Bates C A, Fletcher J R, King P J and Parker L W 1981 *J. Phys. C: Solid State Phys.* **14** L199–206

Abhvani A S, Austen S P, Bates C A, Parker L W and Pooler D R 1982 *J. Phys. C: Solid State Phys.* **15** 2217–31

Abhvani A S, Bates C A, Bury P, King P J, Pooler D R, Rampton V W and Wiscombe P C 1983 *J. Phys. C: Solid State Phys.* **16** 6573–92

Andrianov D G, Suchkova N I, Savel'ev A S, Rashevskaya E P and Filippov M A 1977 *Fiz. Tekh. Poluprovodn* **11** 730–5 (Engl. transl 1977 *Sov. Phys. Semicond.* **11** 426–9

Austen S P, Bates C A and Brugel D 1984 *J. Phys. C: Solid State Phys.* **17** 1257–68

Baker J M 1971 *Rep. Prog. Phys.* **34** 109–73

Barrau J, Brousseau M, Austen S P and Bates C A 1983 *J. Phys. C: Solid State Phys.* **16** 4581–98

Bates C A, Dunn J L and Sigmund E 1987 *J. Phys. C: Solid State Phys.* **20** 1965–83

Berman R, Brock J C F and Huntley D J 1963 *Phys. Lett.* **3** 310–2

Bersuker I B and Polinger V Z 1974 *Zh. Eksp. Teor. Fiz.* **66** 2078–91 (Engl. Transl. 1974 *Sov. Phys.–JETP* **39** 1023–9)

Butler N, Challis L J, Sahraoui-Tahar M, Salce B and Ulrici W 1989a *J. Phys.: Condens. Matter* **1** 1191–203

Butler N, Challis L J, Sahraoui-Tahar M, Salce B, Ulrici W and Cockayne B 1989b *Mater. Sci. Forum* **38–41** 905–10

Butler N, Jouglar J, Salce B, Challis L J, Ramdane A and Vuillermoz P L *Proc. 5th Int. Conf. Phonon Scattering in Condensed Matter (Urbana)* ed A C Anderson and J P Wolfe (Berlin: Springer) pp 123–5

Butler N, Jouglar J, Salce B, Challis L J and Vuillermoz P L 1985 *J. Phys. C: Solid State Phys.* **18** L725–30

Challis L J and de Goër A-M 1984 *The Dynamical Jahn–Teller Effect in Localized Systems* ed Yu E Perlin and M Wagner (Amsterdam: North-Holland) pp 533–708

Challis L J, Locatelli M, Ramdane A and Salce B 1982 *J. Phys. C: Solid State Phys.* **15** 1419–32

Clerjaud B 1985 *J. Phys. C: Solid State Phys.* **18** 3615–61

Cottam R I and Saunders C A 1973 *J. Phys. C: Solid State Phys.* **6** 2105–18
de Wit M and Estle T L 1962 *Bull. Am. Phys. Soc.* **7** 449
Dunn J L and Bates C A 1988 *J. Phys. C: Solid State Phys.* **21** 2495–509
Ennen H, Kaufmann U and Schneider J 1981 *Appl. Phys. Lett.* **38** 355–7
Fujiwara Y, Nishino T and Hamakawa Y 1982 *Japan. J. Appl. Phys.* **21** L727–9
Gehring G A and Gehring K A 1975 *Rep. Prog. Phys.* **38** 1–89
Hamdache M, King P J, Murphy D T and Rampton V W 1982 *J. Phys. C: Solid State Phys.* **15** 5559–80
Hasan F I, King P J, Murphy D T and Rampton V W 1979 *J. Phys. C: Solid State Phys.* **12** L431–3
Kaufmann U and Schneider J 1980 *Advances in Solid State Physics* vol 20 ed J Trensch (Braunschweig: Vieweg) pp 87–116
Lister G M S and O'Brien M C M 1984 *J. Phys. C: Solid State Phys.* **17** 3975–86
Muramatsu S and Iida T 1970 *J. Phys. Chem. Solids* **31** 2209–16
Queisser H J and Theodorou D E 1986 *Phys. Rev.* B **33** 4027–33
Ramdane A, Salce B and Challis L J 1983 *Phys. Rev.* B **27** 2554–7
Ramdane A, Salce B, Challis L J and Locatelli M 1981 *Internal Report* SBT/LCP-81-043, Centre d'Etudes Nucleaires, Grenoble
Rampton V W and Saker M K 1986 *Proc. 5th Int. Conf. Phonon Scattering in Condensed Matter (Urbana)* eds A C Anderson and J P Wolfe (Berlin: Springer) pp 138–40
Sahraoui-Tahar M 1988 *PhD Thesis* University of Nottingham
Sahraoui-Tahar M, Butler N, Challis L J, Salce B and Ulrici W 1989 *Proc. 19th Int. Conf. Physics of Semiconductors (Warsaw 1988)* ed W Zawadski (Warsaw: Polish Academy of Sciences) pp 1019–22
Sakamoto N 1982 *Phys. Rev.* B **26** 6438–43
Salce B 1984 *Proc. 4th Int. Conf. Phonon Scattering in Condensed Matter (Stuttgart 1983)* ed W Eisenmenger, K Lassmann and S Döttinger (Berlin: Springer) pp 58–60
—— 1989 Private communication
Skolnick M S, Brozel M R and Tuck B 1982 *Solid State Commun.* **43** 379–84
Stauss G H and Krebs J 1980 *Phys. Rev.* B **22** 2050–9
Thomas V, Barrau J, Brousseau M, Bates C A, Dunn J L and Ulrici W 1987 *J. Phys. C: Solid State Phys.* **20** 5225–32
Ulrici W, Eaves L, Friedland K, Halliday D P, Kreiss J and Ulrici B 1986 *Mater. Sci. Forum* **10–12** 669–74
Ulrici W and Kreissl J 1988 *Proc. 5th Int. Conf. Semi-Insulating III–V Materials (Malmo)* ed G Crossmann and L Lebedo (Bristol: Adam Hilger) pp 381–6
Zoller W, Dietsche W, Kinder H, de Goër A-M and Salce B 1980 *J. Phys. C: Solid State Phys.* **13** 3591–607